Gravitational waves from compact binaries inspiralling along post-Newtonian accurate eccentric orbits: Data analysis implications

Manuel Tessmer* and Achamveedu Gopakumar†
Theoretisch-Physikalisches Institut, Friedrich-Schiller-Universität Jena, Max-Wien-Platz 1, 07743 Jena, Germany
(Dated: May 23, 2008)

Compact binaries inspiralling along eccentric orbits are plausible gravitational wave (GW) sources for the ground-based laser interferometers. We explore the losses in the event rates incurred when searching for GWs from compact binaries inspiralling along post-Newtonian accurate eccentric orbits with certain obvious non-optimal search templates. For the present analysis, GW signals having 2.5 post-Newtonian accurate orbital evolution are modeled following the phasing formalism, presented in [T. Damour, A. Gopakumar, and B. R. Iyer, Phys. Rev. D **70**, 064028 (2004)]. We demonstrate that the search templates that model in a gauge-invariant manner GWs from compact binaries inspiralling under qudrupolar radiation reaction along 2PN accurate circular orbits are very efficient in capturing our somewhat realistic GW signals. However, three types of search templates based on the adiabatic, complete adiabatic and gauge-dependent complete non-adiabatic approximants, detailed in [P. Ajith, B. R. Iyer, C. A. K. Robinson and B. S. Sathyaprakash, Phys. Rev. D **71**, 044029 (2005)], relevant for the circular inspiral under the qudrupolar radiation reaction were found to be inefficient in capturing the above mentioned eccentric signal. We conclude that further investigations will be required to probe the ability of various types of PN accurate circular templates, employed to analyze the LIGO/VIRGO data, to capture GWs from compact binaries having tiny orbital eccentricities.

PACS numbers: 04.30.Db, 04.25.Nx

I. INTRODUCTION

Compact binaries, namely neutron star–neutron star, black hole–neutron star and black hole–black hole binaries, inspiralling in quasi-circular orbits are the most plausible sources of gravitational radiation for the first generation ground-based laser interferometric gravitational-wave (GW) detectors [1–3]. GW data analysis communities, analyzing noisy data from the operating interferometers, require accurate and efficient temporally evolving GW polarizations, $h_+(t)$ and $h_\times(t)$, the so called GW search templates. In the ongoing efforts to construct GW templates, inspiralling compact binaries are modeled as point particles moving in quasi-circular orbits [4]. The approximation of quasi-circularity in the orbital description while constructing GW templates is quite appropriate, because gravitational radiation reaction quickly reduces the orbital eccentricity as a compact binary evolves towards its last stable orbit (LSO). Employing the dominant contributions to energy and angular momentum losses via GW emission for an inspiralling compact binary, it is straightforward to deduce that when its semi major axis is halved, its eccentricity roughly reduces by a factor of three [5]. The above argument implies that the orbital eccentricity of the Hulse-Taylor binary pulsar when its orbital frequency reaches around 20 Hz will be $\sim 10^{-6}$. Further, it was argued that the templates, constructed to detect GWs from inspiralling compact binaries in quasi-circular orbits should be quite successful in extracting GWs from (mildly) eccentric binaries [6]. Therefore, at present various GW data analysis communities are not explicitly searching for GWs from compact binaries in inspiralling eccentric orbits.

In this paper, we revisit the issue addressed in Ref. [6], namely the possibility of rather efficiently extracting GWs from compact binaries in inspiralling eccentric orbits using search templates constructed for compact binaries evolving in quasi-circular orbits. In our opinion, it is justified to doubt the conclusions of Ref. [6] because it is not that difficult to note that GWs from compact binaries in non-circular orbits were not accurately modeled in Ref. [6], even while restricting the radiation reaction to the dominant order. We observed that dominant secular, but non-reactive, contributions to the orbital evolution were ignored in Ref. [6] (see our Section II for details). Moreover, several astrophysically motivated investigations, carried out in the last few years, indicate that compact binaries in inspiralling eccentric orbits are plausible sources of GWs even for the ground-based GW detectors [7]. Therefore, it is rather important to explore the ability of various types of circular templates to capture somewhat realistic modeling of GWs from compact binaries in inspiralling eccentric orbits. However, we would like to point out that the ability of various types of circular inspiral search templates, available in the LSC Algorithms Library (LAL) [8], to capture GW signals from inspiralling compact binaries having tiny orbital eccentricities will require further investigations. This is due to the fact that in this paper, and following Ref. [6], we only include the dominant contributions to the reactive dynamics.

This paper is organized in the following way. In Section II, we explicate the reasons for our current investiga-

*Electronic address: M.Tessmer@uni-jena.de
†Electronic address: A.Gopakumar@uni-jena.de

tion. Section III presents a brief summary of constructing accurate gravitational waveforms for compact binaries having arbitrary mass ratio moving in inspiralling eccentric orbits. How we revisit the analysis, presented in Ref. [6], is detailed in Section IV and we also present our results in this section. A brief summary, our conclusions and future directions are provided in Section V. Appendix A deals with certain computational details.

II. RESIDUAL ORBITAL ECCENTRICITY AND ITS IMPLICATIONS

The GW signals, namely $h_+(t)$ and $h_\times(t)$, emitted by inspiralling compact binaries can be accurately computed employing the post-Newtonian (PN) approximation to general relativity. The PN approximation to the dynamics of inspiralling compact binaries, usually modeled to consist of point masses, provides, for example, the equations of motion as corrections to the Newtonian one in terms of $(v/c)^2 \sim Gm/c^2\,r$, where v, m and r are the characteristic orbital velocity, the total mass, and the typical orbital separation, respectively. The way any residual orbital eccentricity influences possible loss of event rate for the initial LIGO was explored, for the first time, in Ref. [6]. This was achieved by computing the drops in the signal-to-noise-ratio while searching for GWs from compact binaries moving in inspiralling eccentric orbits with templates constructed for binaries in quasi-circular orbits. The search templates employed in Ref. [6] are essentially given by the following expressions:

$$h_\times(\phi,\omega)|_R = -\,4C\frac{(Gm\eta)}{c^2R'}\left(\frac{Gm\omega}{c^3}\right)^{2/3}\sin 2\phi\,, \qquad (1)$$

where the familiar symbols m and η stand for the total mass and the symmetric mass ratio, while C and R' denote the cosine of the orbital inclination and the radial distance to the binary. The subscript R appearing on the left hand side of Eq. (1) indicates that we are using the so-called restricted PN waveforms as the search templates. The temporal evolution for ϕ and ω, the orbital phase and angular frequency, are governed by

$$\frac{d\phi}{dt} = \omega\,, \qquad (2a)$$

$$\frac{d\omega}{dt} \equiv \frac{\mathcal{L}(\omega)_N}{d\mathcal{E}_N/d\omega} = \frac{96}{5}\left(\frac{G\,\mathcal{M}\,\omega}{c^3}\right)^{5/3}\omega^2\,, \qquad (2b)$$

where $\mathcal{L}(\omega)_N$ and $\mathcal{E}_N$ stand for the dominant contributions to the GW luminosity and the Newtonian orbital energy and the chirp mass $\mathcal{M} \equiv m\,\eta^{3/5}$. Further, it is customary to use $\omega = \pi\,f_{\rm GW}$, $f_{\rm GW}$ being the GW frequency to provide the limits for ω. In the GW literature, Eqs. (1) and (2) provide the 'Newtonian templates' for the quasi-circular inspiral due to the fact that only the dominant contributions to $\mathcal{L}(\omega)$ and $\mathcal{E}(\omega)$ are required to construct $d\omega/dt$. However, it is interesting to note that Eqs. (2) provide certain 2.5PN accurate orbital phase evolution. This observation is due to the fact that in Eqs. (2), one perturbes a compact binary in an exact circular orbit, defined by Eq. (2a), by an expression for $d\omega/dt$, given by Eq. (2b). Therefore, it is reasonable to state that Eqs. (1) and (2) provide a prescription to obtain 2.5PN accurate GW phasing for compact binaries inspiralling along exact circular orbits. We observe that Ref. [6] employed analytically given Fourier domain version of the above search templates (see Eqs. (13), (14) and (15) in Ref. [6]).

Following Ref. [9], there exists two more ways of constructing circular inspiral templates that incorporate the Newtonian reactive dynamics and we detail them below. The orbital phase evolution under the so-called complete adiabatic approximant at the Newtonian order radiation reaction reads

$$\frac{d\phi}{dt} = \omega \equiv \frac{c^3}{G\,m}\,x^{3/2}\,, \qquad (3a)$$

$$\frac{dx}{dt} \equiv \frac{\mathcal{L}(x)_N}{d\mathcal{E}(x)_{2PN}/dx}\,, \text{where} \qquad (3b)$$

$$\mathcal{L}(x)_N = \frac{32\,\eta^2\,c^5}{5\,G}\,x^5\,, \qquad (3c)$$

$$\mathcal{E}(x)_{2PN} = -\frac{\eta\,m\,c^2}{2}\,x\Bigg\{1 - \frac{1}{12}\left[9+\eta\right]x + \left[-\frac{27}{8} + \frac{19}{8}\,\eta - \frac{1}{24}\,\eta^2\right]x^2\Bigg\}. \qquad (3d)$$

The crucial difference between Eq. (2) and (3) is that the numerator in Eq. (3b) is 2PN accurate and the use of the x variable: $x \equiv (G\,m\,\omega/c^3)^{2/3}$. Following Ref. [9], we do not expand the right hand side of Eq. (3b) and therefore, Eqs. (3) also provide a prescription to compute 2.5PN order orbital phase evolution. We recall that in the language of Ref. [9], Eq. (2) provide the adiabatic approximant at the Newtonian order.

The next prescription provides the complete non-adiabatic approximant at the 2.5PN order and following [9], its orbital evolution is defined by

$$\frac{d\phi}{dt} = \omega = \frac{v}{r}\,, \qquad (4a)$$

$$\frac{d\boldsymbol{y}}{dt} \equiv \boldsymbol{v}\,, \qquad (4b)$$

$$\frac{d\boldsymbol{v}}{dt} = -\frac{G\,m}{r^3}\Bigg\{1 - \left[3-\eta\right]\frac{G\,m}{c^2\,r} + \left[6 + \frac{41}{4}\,\eta + \eta^2\right](\frac{G\,m}{c^2\,r})^2\Bigg\}\boldsymbol{y} - \frac{32}{5}\,\eta\,\frac{G^3\,m^3}{c^5\,r^4}\,\boldsymbol{v}\,, \qquad (4c)$$

where $\boldsymbol{y}$ and $\boldsymbol{v}$ define the orbital separation and velocity vectors. It is important to note that the complete non-adiabatic approximant is gauge-dependent and we employed the harmonic gauge in Eqs. (4). Further, note that we are using the circular limit of Eqs. (3.1) to (3.6) in Ref. ([9]) as we are interested in constructing only circular templates.

Let us now take a closer look at the way 2.5PN accurate GW phasing for eccentric binaries, required to model GW signals from compact binaries in inspiralling eccentric orbits, were performed in Ref. [6]. In what follows, first we describe a fully PN accurate prescription to construct the above mentioned GW signals. The process of constructing the expected, and therefore PN accurate, GW signals from compact binaries inspiralling along eccentric orbits, detailed in Ref. [10], is rather involved. To begin with, GW phasing requires an expression, similar to Eq. (1), for $h_\times$. The dominant quadrupolar contribution to $h_\times$, denoted by $h_\times\big|_{\rm Q}$, reads

$$h_\times(r,\phi,\dot r,\dot\phi)\big|_{\rm Q} = -\frac{2Gm\eta C}{c^4 R'}\Bigg[\left(\frac{Gm}{r}+r^2\dot\phi^2-\dot r^2\right)\sin 2\phi - 2\dot r r\dot\phi\cos 2\phi\Bigg], \tag{5}$$

where $\dot r = dr/dt$ and $\dot\phi = d\phi/dt$. When one is interested in doing 2.5PN accurate GW phasing for eccentric binaries, following Ref. [10], it can be argued that the dominant secular reactive evolutions for the dynamical variables, r, ϕ, $\dot r$ and $\dot\phi$, are governed by the following two differential equations:

$$\frac{dn}{dt} = \frac{\xi^{5/3}n^2\eta}{5(1-e_t^2)^{7/2}}\left\{96+292e_t^2+37e_t^4\right\}, \tag{6a}$$

$$\frac{de_t}{dt} = -\frac{\xi^{5/3}n\eta e_t}{15(1-e_t^2)^{5/2}}\left\{304+121e_t^2\right\}, \tag{6b}$$

where $n = 2\pi/T_r$ and e_t are the so-called mean motion and time eccentricity (and T_r being the radial orbital period) and ξ is a shorthand notation for Gmn/c^3. These orbital elements naturally arise in the PN accurate Keplerian type parametric solution to the conservative PN accurate compact binary dynamics, available in Refs. [11–14]. However, the orbital phase of an eccentric binary secularly evolves partly due to the advance of periastron and this effect appears at the first and second PN (conservative) orders. Therefore, in order to have 2.5PN accurate orbital phase evolution, it is imperative to include secular non-radiative effects appearing at the first and second PN orders. In Ref. [10], this is achieved by having the following 2PN accurate expressions for ϕ, symbolically written as

$$\phi = \lambda + W(l;n,e_t)\,, \tag{7a}$$

$$\lambda = (1+k)n(t-t_0)+c_\lambda\,, \tag{7b}$$

$$\text{with}\quad l = n(t-t_0)+c_l\,. \tag{7c}$$

In above equations $k = \frac{\Delta\Phi}{2\pi}$, $\Delta\Phi$ being the advance of periastron in the time interval T_r. Following Ref. [10], we note that $W(l;n,e_t)$ is a 2PN accurate function, given explicitly in terms of eccentric anomaly u, n and e_t and the mean anomaly l is related to u by the 2PN accurate Kepler Equation (KE). The constants t_0, c_l and c_λ refer to some initial instant and values of l and λ at $t = t_0$ (the explicit 2PN accurate expressions for $\lambda(l;n,e_t)$ and $W(l;n,e_t)$ in harmonic gauge is available in Eqs. (25) in Ref. [15]). The reactive secular changes in $\phi(t)$ enter via $n(t)$ and $e_t(t)$ and these time dependencies are governed by Eqs. (6). To be consistent in a PN way, it is also desirable to employ 2PN accurate parameteric equations for $r, \dot r, \phi$ and $\dot\phi$ in terms of n, e_t and $u(l;n,e_t)$ (see Ref. [10] for more details). Therefore to investigate if search templates constructed for compact binaries in quasi-circular orbits, given by Eqs. (1), (2), (3) and (4) are good enough to detect, via matched filtering, GWs from binaries in inspiralling eccentric orbits, it is desirable to model GW signals following Ref. [10]. In other words, GW signals should be constructed incorporating 2.5PN accurate orbital motion in Eq. (5).

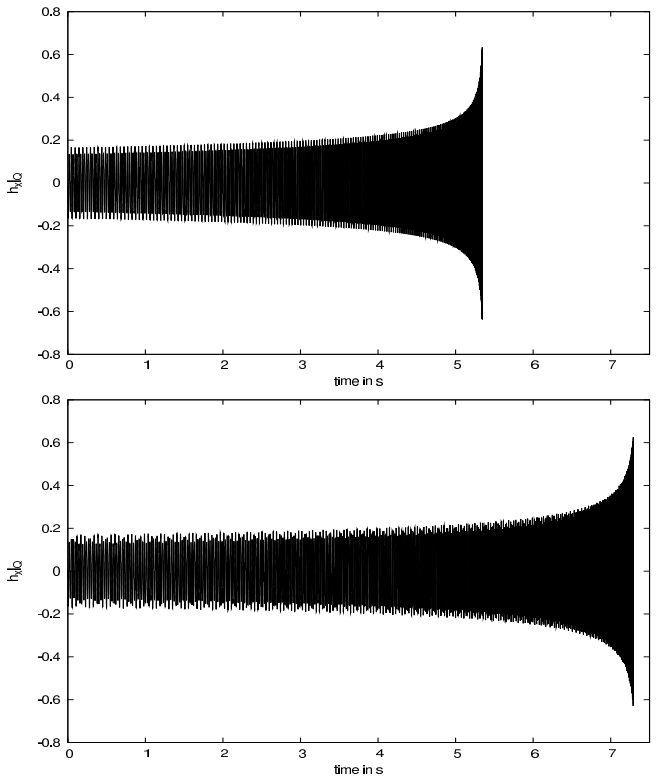

FIG. 1: Plots showing temporal evolution of scaled $h_\times|_Q(t)$, having t in seconds, for $m_1 = 1.4M_\odot, m_2 = 10M_\odot$ and initial $e_t = 0.1$. For the upper plot, orbital motion is governed by Eqs. (6) and (8) and we have $n_i = 125.7$Hz and $n_f = 1211.8$Hz. For the lower plot, the orbital motion is 2.5PN accurate and $n_i = 111.7$Hz and $n_f = 741.0$Hz, obtainable with the help of Eq. (9). The two sets of initial and final n values result from the fact that for both cases quadrupolar f_{GW} can only vary between 40Hz and $(6^{3/2}\pi G m/c^3)^{-1}$. Further, notice the visible effect of k in the lower plot.

However, this is not the way GWs from inspiralling eccentric orbits are modeled in Ref. [6] and one can summarize their inaccurate construction of GW signals in the following way. We observe that Ref. [6] essentially employs the same expression for $h_\times|_{\rm Q}$, but descriptions for conservative $r, \dot r, \phi$ and $\dot\phi$ were purely Newtonian and ra-

diation reaction enters via Eqs. (2) (we recall that Ref. [6] employs different orbital variables to describe the binary dynamics and therefore required to solve numerically three coupled differential equations). The crucial difference with respect to what is done in Ref. [10] is that the secular 1PN and 2PN corrections to the orbital phase evolution were neglected in Ref. [6]. The conservative orbital dynamics pursued in Ref. [6] may be defined in terms of Keplerian parameterization and it reads

$$r = \left(\frac{Gm}{n^2}\right)^{1/3} (1 - e_t \cos u)\,, \tag{8a}$$

$$\dot{r} = \frac{e_t (Gmn)^{1/3}}{(1 - e_t \cos u)}\, \sin u\,, \tag{8b}$$

$$\phi = \lambda + W(l) = n(t - t_0) + (v - u) + e_t \sin u\,, \tag{8c}$$

$$\dot{\phi} = \frac{n\sqrt{1 - e_t^2}}{(1 - e_t \cos u)^2}\,, \tag{8d}$$

$$\text{where}\quad v - u = 2\tan^{-1}\left(\frac{\beta \sin u}{1 - \beta \cos u}\right)\,, \tag{8e}$$

and β being $(1 - \sqrt{1 - e_t^2})/e_t$. In above expressions, u, v and e_t are the usual eccentric and true anomalies and Newtonian orbital eccentricity of the Keplerian parameterization. The reactive evolution (again) is governed by Eqs. (6) and the explicit temporal evolution of $h_\times|_Q(t)$ also requires numerical solution of classical Kepler Equation $l \equiv n(t - t_0) = u - e_t \sin u$. The above mentioned two approaches to obtain $h_\times|_Q(t)$ lead to quite different GW signals for compact binaries moving in inspiralling eccentric orbits as demonstrated in Fig. 1. For $h_\times|_Q(t)$, constructed following Ref. [10], one can clearly observe secularly changing modulations due to periastron advance. Another feature to note is that $h_\times|_Q(t)$, having 2.5PN accurate orbital motion, lasts longer than $h_\times|_Q(t)$ having Eqs. (6) imposed on Newtonian accurate orbital motion. This is mainly because of using different n_i and n_f, initial and final values for n, for the two cases. This is required to make sure that the initial and final frequencies of the emitted quadrupolar GWs are 40 Hz and $(6^{3/2}\,\pi\, Gm/c^3)^{-1}$ for our two cases (recall that advance of periastron shifts the dominant harmonic as explained in Ref. [16]). Further, while constructing these figures, we assume that first and third harmonics are irrelevant for the initial LIGO. In our opinion, astrophysical GWs from compact binaries in inspiralling eccentric orbits are rather more accurately (and realistically) modeled in Ref. [10] compared to Ref. [6] and therefore, we are justified to doubt conclusions presented in Ref. [6]. However, it is important to note that in a purely GW data analysis sense, while employing Eqs. (5), (6) and (8) to model GWs from inspiralling eccentric binaries, the conclusions of Ref. [6] are indeed correct. This allowed us to accurately calibrate our codes with the results presented in Ref. [6].

We are now in a position to explore if the various circular templates, given by Eqs. (1), (2), (3) and (4), are going to efficient in capturing GWs from eccentric binaries. Because the matched filtering requires accurate secular description for GW phase evolution, this can roughly be done by computing and comparing (for the various cases under study) $\mathcal{N}_{GW}$, the number of accumulated GW cycles between some minimum and maximum GW frequencies. Making use of the definition $\mathcal{N}_{GW} = (\phi_{\rm max} - \phi_{\rm min})/\pi$, where $\phi_{\rm max}$ and $\phi_{\rm min}$ are the values of the orbital phase associated with the some minimum and maximum GW frequencies, we can easily evaluate the $\mathcal{N}_{GW}$ associated with an approximant in the time-domain. We list below the various cases involved in the present study, where the reactive effects are restricted to the dominant quadrupolar contributions.

- Case I: The adiabatic approximant and the associated search templates are given by Eqs. (1) and (2).
- Case II: The complete adiabatic circular inspiral and the associated search templates are specified by Eqs. (1) and (3).
- Case III: The gauge-dependent complete non-adiabatic circular inspiral and the associated search templates are specified by Eqs. (1) and (4).
- Case IV: The eccentric $h_\times(t)$, given by Eqs. (5), (8) and (6) and this is the GW signal employed in Ref. [6].
- Case V: The eccentric $h_\times(t)$, given by Eqs. (5) and where the 2.5PN accurate orbital phase evolution is computed following Ref. [10].
- Case VI: The newly introduced circular templates given by Eqs. (19) and (20),

We would like to point out that Ref. [6] investigated a scenario involving the cases IV and I. In this study, we use the case V to model the fiducial GWs from an eccentric binary and employ the cases I, II, III and VI to construct the inspiral templates[recall that cases II, III and VI do incorporate in different ways 2PN accurate conservative dynamics to construct the search templates]. The use of the case I to model search templates in our comparison is based on the following two arguments. The first is that, strictly speaking and as explained earlier, Eqs. (2) also describe 2.5PN accurate orbital phase evolution of a compact binary inspiralling along exact circular orbits, defined by Eq. (2a). The second reason is that we would like to probe the performances of all the three types of search templates, introduced in Ref. [9] and having quadrupolar reactive dynamics, while treating the case V to model GWs from eccentric binaries.

Let us briefly explain how we perform the $\mathcal{N}_{GW}$ computations in the time-domain for the various cases. For the case I, we use $40\,\pi$Hz and $\left(6^{3/2}\,Gm/c^3\right)^{-1}$ as the initial and final values of ω for the temporal evolution defined by Eqs. (2) and similar limits also apply to the case

II. The difference in ϕ at the above two ω values leads to $\mathcal{N}_{GW}$ for the cases I and II. For the case III, we need to specify r and v values associated with the above mentioned ω limits and we use 2PN accurate expression for ω in terms of r, given by Eq. (3.11) in Ref. [24], to obtain the relevant limits for r and $v = \omega\, r$. For the Newtonian accurate conservative and eccentric orbital motion, treated as the case IV, the lower and upper values of n, n_i and n_f, are identified with the above mentioned ω limits due to the fact that at this order $n = \omega$. Further, reactive evolution is given by Eqs. (6) and the values of ϕ, obtained by using relevant parts of Eqs. (8) and the classical KE, evaluated at the instances when n reaches the values n_i and n_f lead to $\mathcal{N}_{GW}$ for the case IV. For the case V, the values for n_i and n_f are numerically obtained by using the following 2PN accurate relation

$$\pi\, f_{\rm GW} = n\Bigg\{1 + \frac{3\xi^{2/3}}{1-e_t^2} + \frac{\xi^{4/3}}{4(1-e_t^2)^2}\Bigg[78 - 28\eta + (51-26\eta)e_t^2\Bigg]\Bigg\}. \tag{9}$$

This is justified because of the observation in Ref. [16] that the dominant GW spectral component of a mildly eccentric compact binary, having PN accurate orbital motion, appears at $(1+k)\, n/\pi$. Using $\omega_i = 40\,\pi$Hz and $\omega_f = \left(6^{3/2}\, Gm/c^3\right)^{-1}$, it is easy to obtain numerically n_i and n_f for the three canonical binaries considered in Table I. Using 2.5 PN accurate $\phi(l; n, e_t)$ in harmonic gauge, obtainable using Eqs. (25) and (27) in Ref. [15] and Eqs. (6), we compute values of $\phi(t)$ at instances when n reaches its above mentioned limiting values as $\phi_{\rm min}$ and $\phi_{\rm max}$. It is not very difficult to infer that we can choose, without any loss of generality, $\phi_{\rm min} = 0$ at $t = 0$ in all cases of $\mathcal{N}_{GW}$ evaluations. Finally, for the case VI, the limiting values for n are obtained using the circular limit of Eq. (9) and a procedure similar to the case I to compute the relevant $\mathcal{N}_{GW}$.

The resulting GW cycles, $\mathcal{N}_{GW}$, for three typical compact binaries computed using the above mentioned six different prescriptions are listed in Table I. We observe that the differences in $\mathcal{N}_{GW}$ between cases I and IV are not very large. This indicates that quasi-circular templates, given by Eqs. (1) and (2), should be highly efficient to pick up GW signals modeled using Eqs. (5), (6) and (8) for small values of initial eccentricities. We also observe that for a given e_t the differences in $\mathcal{N}_{GW}$ between the cases I and IV decrease as we increase the total mass. This is also consistent with the observation in Ref. [6] that for high mass binaries eccentricities up to 0.2 may be tolerated while searching with quasi-circular templates. However, the differences in $\mathcal{N}_{GW}$ between the cases I, II, III and V are quite large even when initial $e_t \sim 0.01$. This makes it interesting to revisit the analysis performed in Ref. [6]. However, the differences in $\mathcal{N}_{GW}$ between the cases V and VI indicate that the new type of circular inspiral templates, given by Eqs. (19) and (20), should be more efficient in capturing our somewhat realistic eccentric GW signals. In the next section, we briefly summarize 2.5PN accurate GW phasing, available in Ref. [10], and present a prescription to perform it in a highly accurate and efficient manner.

TABLE I: The accumulated number of GW cycles, $\mathcal{N}_{GW}$, relevant for the initial LIGO, while considering the above detailed six types of orbital phase evolutions for the three types of canonical binaries. We recall that the radiation reaction is always restricted to the dominant quadrupolar order.

$m_1/M_\odot : m_2/M_\odot$	1.4 : 1.4	1.4 : 10	10 : 10
Case I			
$e_t \equiv 0$	1587.0	347.4	56.5
Case II			
$e_t \equiv 0$	1517.7	305.8	46.6
Case III			
$e_t \equiv 0$	1487.8	295.9	46.3
Case IV			
$e_t = 0.01$	1587.0	347.4	56.5
$e_t = 0.05$	1575.8	344.9	56.1
$e_t = 0.10$	1541.8	337.3	54.8
Case V			
$e_t = 0.01$	1829.5	497.8	91.9
$e_t = 0.05$	1817.3	494.7	91.4
$e_t = 0.10$	1779.2	485.1	89.6
Case VI			
$e_t \equiv 0$	1830.5	497.4	91.9

III. ACCURATE GW PHASING FOR ECCENTRIC BINARIES AT 2.5PN ORDER

In what follows, we briefly summarize a prescription to efficiently perform 2.5PN accurate GW phasing for compact binaries of arbitrary mass ratio moving along inspiralling eccentric orbits presented in Ref. [10]. The temporal evolution of the dynamical variables, $r(t)$, $\dot{r}(t)$, $\phi(t)$ and $\dot{\phi}(t)$, appearing in Eq. (5) for $h_\times|_Q(t)$, is achieved by employing a version of the general Lagrange method of variation of arbitrary constants. The idea is to split the compact binary dynamics, defined by the relative acceleration $\mathcal{A}$, into two parts. In general, $\mathcal{A}$ consists of a conservative, and in our case integrable, part $\mathcal{A}_0$ and a reactive part $\mathcal{A}'$ that perturbes the conservative dynamics. To perform efficient GW phasing, we employ a "semi-analytic" solution to the conservative dynamics $\mathcal{A}_0$. Thereafter, a solution to the PN accurate dynamics $\mathcal{A} = \mathcal{A}_0 + \mathcal{A}'$ is obtained by varying the constants present in the generic solution to $\mathcal{A}_0$.

In the present paper, we restrict $\mathcal{A}_0$ to be 2PN accurate and $\mathcal{A}'$ contains only the dominant 2.5PN contributions, the so called Newtonian RR terms. When the conservative binary dynamics is 2PN accurate, it is convenient to express the relative separation vector $\boldsymbol{r}$ (in a suitably defined 'center-of-mass frame') as

$$\boldsymbol{r} = r\, \cos\phi\, \vec{\mathbf{i}} + r\, \sin\phi\, \vec{\mathbf{j}}, \tag{10}$$

where $\vec{\mathbf{i}} = \vec{\mathbf{p}}$, $\vec{\mathbf{j}} = \cos i\, \vec{\mathbf{q}} + \sin i\, \vec{\mathbf{N}}$ [note that $(\vec{\mathbf{p}}, \vec{\mathbf{q}}, \vec{\mathbf{N}})$ is the same orthonormal triad employed to construct $h_\times|_Q$]. The 2PN accurate expressions for the dynamical variables $r(t)$, $\phi(t)$ and their time derivatives may be expressed parametrically as

$$r(t) = r\ (u(l), n, e_t) \tag{11a}$$
$$\dot{r}(t) = \dot{r}\ (u(l), n, e_t) \tag{11b}$$
$$\phi(t) = \lambda(t, n, e_t) + W(u(l), n, e_t) \tag{11c}$$
$$\dot{\phi}(t) = \dot{\phi}\ (u(l), n, e_t) \tag{11d}$$

The explicit 2PN accurate expressions for the above quantities in harmonic gauge, employed in this paper, can be extracted from Eqs. (23), (24), (25) and (26) in Ref. [15] and they are explicitely provided in appendix A. The basic angles l and λ, symbolically given in Eq. (7) [see Eqs. (25) and (27) of Ref. [15] for the 2PN accurate explicit expressions], read

$$l = n\,(t - t_0) + c_l\,, \tag{12a}$$
$$\lambda = (1 + k)\, n\,(t - t_0) + c_\lambda\,. \tag{12b}$$

The explicit time evolutions for $r, \dot{r}, \phi$ and $\dot{\phi}$ are provided by the following 2PN accurate Kepler equation, in harmonic gauge, which connects l and u (see Eq. (27) in Ref. [15]):

$$\begin{aligned} l = {} & u - e_t \sin u \\ & + \frac{\xi^{4/3}}{8\sqrt{1-e_t^2}(1 - e_t \cos u)} \Big\{ (15\eta - \eta^2) e_t \sin u \sqrt{1 - e_t^2} \\ & + 12(5 - 2\eta)(v - u)(1 - e_t \cos u) \Big\}\,. \end{aligned} \tag{13}$$

In the above description for the conservative 2PN accurate dynamics, we have four constants of integration, namely n, e_t, c_l and c_λ. When the orbital dynamics is fully 2.5PN accurate, i.e., $\mathcal{A} = \mathcal{A}_0 + \mathcal{A}'$, then the above four constants of integration become time dependent. The differential equations governing the four constants of integration can be computed by demanding same functional forms for $r, \dot{r}$ and $\dot{\phi}$ even when the binary dynamics is fully 2.5PN accurate. Further, following Ref. [10], the temporal evolution in each n, e_t, c_l and c_λ can be treated to consist of a slow drift component and a rapidly oscillating part. Symbolically, the above mentioned split in the four variables reads

$$c_\alpha(t) = \bar{c}_\alpha(t) + \tilde{c}_\alpha(t)\,, \tag{14}$$

where α denotes one of the four constants of 2PN accurate orbital dynamics, namely, n, e_t, c_l and c_λ. To our desired PN order, it was demonstrated in Ref. [10] that $d\bar{c}_l/dt = d\bar{c}_\lambda/dt = 0$ and $d\bar{n}/dt$ and $d\bar{e}_t/dt$ are given by Eqs. (6). For the current (and preliminary) numerical investigations, we neglected small amplitude fast oscillations $\tilde{n}, \tilde{e}_t, \tilde{c}_\lambda$ and $\tilde{c}_l$ (however, their explicit expressions in harmonic gauge may be obtained from Eqs. (36) in Ref. [15]). To do GW phasing, we proceed as follows. Using 2PN accurate expressions for $r, \dot{r}, \phi$ and $\dot{\phi}$ and 2PN accurate Kepler equation, extractable from Eqs. (23)-(27) in Ref. [15], we compute $r(t), \dot{r}(t), \phi(t)$ and $\dot{\phi}(t)$ using n and e_t to represent our PN accurate eccentric orbit. After that, we numerically impose reactive evolutions in $e_t(t)$ and $n(t)$, defined by Eqs. (6), on the 2PN accurate orbital dynamics and compute the associated $h_\times|_Q(t)$ using Eq. (5). This is how we compute $h_\times|_Q(t)$ with PN accurate orbital evolution.

From the above discussions, it is clear that an efficient implementation of GW phasing also depends on an efficient (and accurate) way of solving the 2PN accurate Kepler Equation. This is achieved by employing a slightly modified method of Mikkola to solve the classical Kepler Equation. This is detailed in the next subsection.

A. Mikkola's solution adapted to 2PN accurate Kepler Equation

There exists a plethora of analytical and numerical solutions associated with the celebrated classical KE, namely $l \equiv n(t - t_0) = u - e_t \sin u$ (see Ref. [17]). Arguably the most accurate and efficient numerical way to solve the classical KE is by Seppo Mikkola [18]. Therefore, we adapt Mikkola's simple and robust method to solve our 2PN accurate KE, given by Eq. (13). Let us now we briefly discuss Mikkola's procedure. Recall that a numerical solution to the KE usually employs Newton's method which requires an initial guess u_0 that depends on l and e_t. A number of iterations will be required to obtain an approximate solution that has some desired accuracy. The number of iterations to reach this accuracy naturally depends on u_0, e_t and l.

In Mikkola's method, u_0 is computed by introducing a new auxiliary variable $s = \sin u/3$. The resulting equation for s is Taylor expanded, forming a cubic polynomial in s. The resulting approximate solution is empirically corrected to negate the largest error occurring at $l = \pi$ leading to a u value which has an accuracy of not less than 10^{-3}. This accuracy is greatly enhanced by employing a fourth order version of Newton's method (see Ref. [18] for further details). This procedure provides u as a function of l within an accuracy of 10^{-15} for all values of e_t and l for $e_t \in (0, 1)$. We note that the above method requires reduction of l into the interval $-\pi \leq l \leq \pi$ in order to make s as small as possible. It is possible to employ geometrical interpretations of u and l, to map any l in to the above interval, as explained in Ref. [16]. We note, while passing, that Mikkola's solution only demands the solution of a cubic polynomial that involves no trigonometric functions and one-time evaluation of a couple of simple trigonometric functions.

To solve the fully 2PN accurate KE, we apply Mikkola's method at various PN orders in a successive manner in the following way. First we solve the 1PN accurate KE, $l = n(t - t_0) = u - e_t \sin u$, via Mikkola's

method, and obtain u (note that due to the use of e_t both 1PN and Newtonian accurate Kepler Equations have identical structure and hence solutions). This allows us to obtain 2PN corrections appearing on the right hand side of Eq. (13) for l in terms of (n, e_t, l) and let us denote it by l_4. We obtain the solution to 2PN accurate KE by introducing $l' = l - l_4 = u - e_t \sin u$ and applying Mikkola's scheme to obtain $u(l')$. This allows us to get accurate and efficient solution to 2PN accurate KE that provides u in terms of l, e_t, n, m and η.

We are now in a position to explore data analysis implications of $h_\times|_Q(t)$ having 2.5PN accurate orbital motion.

IV. NONOPTIMAL MATCHED FILTER SEARCHES FOR GW SIGNALS HAVING SOME RESIDUAL ECCENTRICITIES

In this section, we explore the implications for initial LIGO if $h_\times\big|_{\rm Q}(t)$, given by Eq. (5), evolving under 2.5PN accurate orbital motion, represents a potential GW signal. This is done by revisiting the analysis done in Ref. [6].

GW data analysts employ the technique of 'matched filtering' to search for GWs from compact binaries. This is an optimal technique provided one can construct search templates that accurately model expected signals from GW sources, especially in their phase evolution. It is natural that these templates depend on a number source parameters and therefore one needs to construct a 'bank of templates' that densely covers the parameter space of a specific (and desired) GW source. The efficiency of a specific template bank in detecting the associated GW sources is expressed by computing its Fitting Factor (FF), which is a measure of the 'overlap' between the expected GW signal and its approximate model, given by a template in the template bank [19]. If a template bank can provide FFs ~ 1, one can be confident about the possible detection of the associated GW signals. Further, it was pointed out in Ref. [19] that the loss in event rate due to the deployment of inaccurate templates is $\propto 1$ - FF^3. And, the typical desirable FFs for initial LIGO are ≈ 0.97 [20].

Following Refs. [6, 19], we compute FFs in the following way. Let GW signals from compact binaries inspiralling along non-circular orbits be denoted by $s(t)$ and let the associated quasi-circular templates be $h(t;\boldsymbol{\lambda})$, where $\boldsymbol{\lambda}$ stands for template parameters. Further, let $\tilde{s}(f)$ and $\tilde{h}(f;\boldsymbol{\lambda})$ denote Fourier Transforms of $s(t)$ and $h(t;\boldsymbol{\lambda})$, computed by employing 'realft' routine of [21]. With these inputs and following Ref. [19], we define the ambiguity function $\mathcal{A}(\boldsymbol{\lambda})$ as

$$\mathcal{A}(\boldsymbol{\lambda}) = \frac{(s|h(\boldsymbol{\lambda}))}{\sqrt{(s|s)(h(\boldsymbol{\lambda})|h(\boldsymbol{\lambda}))}}\,, \tag{15}$$

where the matched filter inner product $(a|b)$ by definition reads

$$(a|b) = 2\int_0^\infty \frac{\tilde{a}^*(f)\tilde{b}(f) + \tilde{a}(f)\tilde{b}^*(f)}{S_n(f)}\,df\,. \tag{16}$$

In the above expression, $S_n(f)$ stands for the one sided noise power spectral density of the detector and we have for the initial LIGO

$$\begin{aligned} S_n(f) =& S_0[(4.49x)^{-56} + 0.16x^{-4.52} + 0.52 \\ &+ 0.32x^2], \quad f \geq f_s\,, &\text{(17a)}\\ =& \infty, \quad f < f_s\,, &\text{(17b)}\end{aligned}$$

where $x = f/f_0$, with $f_0 = 150$Hz and $f_s = 40$Hz. The constant S_0 never enters our computations and hence its value is irrelevant for us. When one employs quasi-circular templates, given by Eqs. (1) and (2), it is possible to separate $\boldsymbol{\lambda}$ into $\boldsymbol{\lambda} = (t_0, \phi_0, \boldsymbol{\theta})$, where t_0 and ϕ_0 denote the time of arrival and the associated orbital phase of the binary and $\boldsymbol{\theta}$ denotes the remaining parameters. Following Ref. [19], one can easily maximize $\mathcal{A}$ over t_0 and ϕ_0 while employing 'realft' routine to compute $\tilde{s}(f)$ and $\tilde{h}(f,\boldsymbol{\lambda})$. The FF is the maximum value of the ambiguity function, i.e, FF $\equiv \max_{\boldsymbol{\lambda}} \mathcal{A}(\boldsymbol{\lambda})$. For circular templates, defined by Eqs. (1) and (2), the only component of $\boldsymbol{\theta}$ is the chirp mass $\mathcal{M}$ and therefore

$$FF = \max_{t_0,\phi_0,\mathcal{M}} \mathcal{A}(\boldsymbol{\lambda})\,. \tag{18}$$

However, while employing the cases II, III and IV to model the circular templates, it is clear that the above maximization has to be performed over m and η. For these cases, we invoked the mini-max overlap, detailed in Ref. [22], and the 'amoeba' routine of Ref. [21] to compute the associated FFs. Below we describe how we tackled the analysis performed in Ref. [6].

A. Brief summary of how we revisited the analysis of Ref. [6]

Let us first briefly describe how GW signals were actually constructed in Ref. [6]. They employed Newtonian accurate conservative orbital evolution and imposed on it the adiabatic evolution of orbital elements arising from Einsteinian quadrupole formulae for the energy and angular momentum fluxes. The actual construction of GW signals from compact binaries in inspiralling eccentric orbits was achieved by employing semi-latus rectum p and eccentricity e to describe the Newtonian accurate (conservative) orbital motion. The effects of radiation reaction were incorporated by employing coupled differential equations for dp/dt and de/dt, computed using energy and angular momentum balances. We note that in Ref. [6] the construction of the GW signal, $s(t) = h_\times\big|_{\rm Q}(t)$, required solving numerically three coupled differential equations, namely, those for $d\phi/dt, dp/dt$ and de/dt (see Eqs. (6), (8) and (9) in Ref. [6]). Further,

Ref. [6] computed frequency domain versions of Newtonian accurate quasi-circular templates, using the stationary phase approximation [see their Eqs. (13) and (14) and (15)].

To repeat the analysis of Ref. [6], we constructed GW signals by employing Eqs. (5) for $h_\times|_Q(t)$, Eqs.(8) for the purely Newtonian accurate conservative orbital motion and Eqs. (6) to impose the effects of radiation reaction on the orbital motion. Therefore, our prescription leads to solving numerically coupled differential equations for n and e_t along with the classical Kepler Equation. Our quasi-circular templates are given by Eqs. (1) and (2) and we employed the 'realft' routine to compute $\tilde{s}(f)$ and $\tilde{h}(f,\boldsymbol{\lambda})$. For a given initial eccentricity, initial value for mean motion $n = 2\,\pi/T$ is chosen following Ref. [16], which provided a detailed spectral analysis for GWs from eccentric binaries. This allowed us to choose, for Newtonian binaries of all masses, $n_i = 125.7$Hz when $e_i = 0.01$, the initial value for e_t, and $n_i = 83.8$Hz for $e_i = 0.1$. Note that in Ref. [6], initial orbital frequency was always chosen to be $40/3 = 13.3$Hz, where 40Hz being the lower frequency cut-off for the initial LIGO. This is mainly due to the assumption of Ref. [6] that GWs from eccentric binaries can be decomposed into components that oscillate at once, twice and thrice the orbital (radial) frequency. We let the final value for n be $(6^{3/2}\,G\,m/c^3)^{-1}$ as compact binaries that we considered here were circularized when n reached the above value and because $n = \omega$ at Newtonian order. Further, in most FF computations, the search templates were chosen to evolve in a GW frequency window having 40Hz and $(6^{3/2}\,\pi\,Gm/c^3)^{-1}$ as their lower and upper limits. We noted that our results were somewhat insensitive to minor changes in n_f. We are aware that Ref. [6] employed h_+ for their FF computations. However, we choose $h_\times$ mainly because we can factor out $-2\,G\,m\,C/(c^2R')$ from our GW signals and templates.

Employing the above mentioned procedure and restricting the initial values of $e_t \leq 0.1$, we were able to reproduce most of the entries in Tables II and III of Ref. [6]. This gave us a lot of confidence in our routines to implement the FFs. In the next subsection, we detail the FF computations that employ Eq. (5) having 2.5PN accurate orbital evolution to model GWs from eccentric binaries, while employing the cases I, II, III and VI as the search templates to probe the performances of these circular templates.

B. Fitting Factor computations involving the cases I, II, III, V and VI

In this section, first, we present the results from our FF computations that employ Eq. (5) having 2.5PN accurate orbital evolution, detailed in the Section III, to model, somewhat realistically, GWs from inspiralling eccentric binaries. And, we employ as search templates the three types of circular waveforms, given by Eqs. (1) and (2), Eqs. (1) and (3) and Eqs. (1) and (4) [and these are the above detailed cases I, II and III]. In other words, we are exploring if the adiabatic, complete adiabatic and gauge-dependent complete non-adiabatic circular templates, having reactive evolution restricted to the dominant qudrupolar order will be efficient to capture our fiducial eccentric signal, detailed in Section III. We are aware that comparing the cases V and I may be objectionable due to the use of Newtonian accurate quantities in the derivation of the right hand side of Eq. (2b). However, and as mentioned earlier, we pursued such a comparison due to the following two reasons. First, it is interesting to note, from a strict PN point of view, that Eqs. (2) also provide 2.5PN order GW phase evolution. Secondly, we want to explore whether the various types of circular templates, detailed in Ref. [9], can capture our somewhat realistic eccentric $h_\times(t)$. We would like to emphasize that a similar objection is *not* applicable while employing the cases II and III to model circular templates. The FFs, relevant for the initial-LIGO, for the cases I, II and III while employing Eq. (5) having 2.5PN accurate orbital phase evolution to model the fiducial eccentric GW signals are listed in Table II.

Significantly lower FFs, listed in Table II, clearly indicate that GW templates, defined by Eqs. (1), (2), (3) and (4) are not efficient in capturing our somewhat realistic GW signals. For the sake of completeness, we note that FF computations that used GW signals having lower values of initial e_t also gave us similar lower numbers [we note that it is rather difficult (numerically) to use values below 10^{-3} for initial eccentricities in our GW signals construction]. However, low FFs are consistent with the arguments, based on the number of accumulated GW cycles, presented in Section II.

Let us now explain the way we constructed the inspiral templates associated with the case VI. The new circular inspiral template family is obtained by taking the circular limit, defined by $e_t \to 0$, of Eqs. (6), (26), (48d), (51), (52), (53) and (63) in Ref. [10]. Using these expressions in the limit $e_t \to 0$, we constructed a new type of GW templates for compact binaries inspiralling along PN accurate quasi-circular orbits. The relevant expressions are

$$h_\times(\phi,n)|_R = -4C\frac{(Gm\eta)}{c^2R'}\left(\frac{Gmn}{c^3}\right)^{2/3}\sin 2\phi\,, \qquad (19)$$

where $\phi(t)$ and $n(t)$ are governed by

$$\frac{d\phi}{dt} = n\left\{1 + 3\,\xi^{2/3} + \left(\frac{39}{2} - 7\,\eta\right)\,\xi^{4/3}\right\}, \qquad (20a)$$

$$\frac{dn}{dt} = \frac{96}{5}\,\eta\,\left(\frac{Gmn}{c^3}\right)^{5/3} n^2\,. \qquad (20b)$$

In our expression for $h_\times(\phi,n)|_R$ we have neglected PN corrections to $G\,m/r$ and $\dot{\phi}$ in the $e_t \to 0$ limit. This is justified as we can treat these corrections forming PN contributions to the amplitude of $h_\times$ (this is indeed the way PN corrections to $h_\times$ and h_+ were computed in

TABLE II: The FFs, relevant for the initial-LIGO, involving the adiabatic, complete adiabatic and gauge-dependent complete non-adiabatic approximants, namely the cases I, II and III, as search templates and where the reactive order is at the dominant quadrupolar level. The fiducial eccentric signals are constructed using Eq. (5) where the orbital dynamics is fully 2.5PN accurate [the case V]. The templates that provide the listed FFs are characterized by $\mathcal{M}_t$, m_t and η_t. We do not employ the third harmonic while modeling our eccentric GW signals.

$m_1/M_\odot : m_2/M_\odot$		1.4 : 1.4	1.4 : 10	10 : 10
Case V Vs Case I				
$e_t = 0.01$	FF	0.533	0.509	0.655
	$\mathcal{M}_t/\mathcal{M}_s$	0.910	0.802	0.745
$e_t = 0.05$	FF	0.532	0.507	0.654
	$\mathcal{M}_t/\mathcal{M}_s$	0.910	0.802	0.744
$e_t = 0.10$	FF	0.522	0.507	0.659
	$\mathcal{M}_t/\mathcal{M}_s$	0.912	0.803	0.746
Case V Vs Case II				
$e_t = 0.01$	FF	0.430	0.504	0.755
	m_t/m_s	0.870	0.622	0.614
	η_t/η_s	0.992	1.366	0.987
$e_t = 0.05$	FF	0.428	0.500	0.744
	m_t/m_s	0.877	0.655	0.659
	η_t/η_s	0.980	1.250	0.863
$e_t = 0.10$	FF	0.417	0.493	0.732
	m_t/m_s	0.900	0.689	0.623
	η_t/η_s	0.939	1.151	0.934
Case V Vs Case III				
$e_t = 0.01$	FF	0.424	0.500	0.772
	m_t/m_s	0.852	0.580	0.601
	η_t/η_s	1.000	1.492	0.997
$e_t = 0.05$	FF	0.420	0.494	0.762
	m_t/m_s	0.886	0.678	0.662
	η_t/η_s	0.936	1.139	0.836
$e_t = 0.10$	FF	0.411	0.487	0.752
	m_t/m_s	0.889	0.737	0.603
	η_t/η_s	0.935	0.984	1.000

Ref. [23]). We detail below various properities of this new approximant.

It is interesting to note that, in the PN approximation and while dealing with the restricted PN waveforms, Eqs. (19) and (20) are simply another representation of Eqs. (1) and (2). In other words, both Eqs. (1) and (2) and Eqs. (19) and (20) can be used to describe GWs from quasi-circular compact binaries having 2.5PN accurate non-stationary orbital phase evolution. The difference is that the use of $d\phi/dt \equiv \omega$ leads to a PN independent stationary phase evolution and while in terms of n, it is evidently PN dependent. Further, following [12], one can also demonstrate that n is indeed a gauge invariant PN accurate quantity like ω. Therefore, based on purely theoretical arguments, it is not possible to argue against the use of n to construct quasi-circular PN accurate GW search templates. In principle, one can employ other gauge invariant quantities like the orbital energy or angular momentum to construct GW search templates. We have used n in Eqs. (19) and (20) as 2.5PN accurate GW phasing for eccentric binaries, available in Ref. [10], employed n. And, what are the most appropriate variables to do perform accurate GW phasing for eccentric binaries will be reported elsewhere.

A rather confusing consequence of expressing $d\phi/dt = \omega = n(1+k)$ in terms of n for the quasi-circular inspiral is the following. The PN accurate conservative angular motion becomes $\phi - \phi_0 = n\,(1+k)\,(t-t_0)$. Therefore, deviations from the Newtonian accurate angular motion can be attributed the rate of periastron advance. This is despite of the fact that for circular orbits, it is rather difficult to visualize the periastron advance. However, if one employs, for example, the orbital energy to prescribe the orbit, it is no more possible to make the above statement as both n and k are PN accurate functions of the orbital energy. We note that similar arguments and expressions were employed in Ref. [24] during the PN accurate GW phasing of quasi-circular inspiral [see Eqs. (4.20)–(4.24) in Ref. [24] and the appendix A].

Finally, we would like to point out that Eqs. (20) also represent an adiabatic inspiral. This is because the balance arguments, similar to the ones employed in the derivation of $d\omega/dt$ and dx/dt, are also required to compute dn/dt. In contrast, in the complete non-adiabatic approximant, one does not require to invoke any balance arguments. Further, it is possible to provide the following physical explanation for the new template family. One may state that Eqs. (19) and (20) model GWs from a compact binary in a 2PN accurate circular orbit, defined by Eq. (20a), perturbed by the dominant order radiation reaction, given by Eq. (20b). We would like to recall that in Ref. [10], the phasing for eccentric binaries were performed by perturbing compact binaries in PN accurate eccentric orbits by appropriate PN accurate reactive dynamics for eccentric binaries.

Therefore, we repeated our above mentioned FF computations using $h(t, \boldsymbol{\lambda})$, given by Eqs. (19) and (20) and we again employed the 'realft' routine to compute the associated $\tilde{s}(f)$ and $\tilde{h}(f, \boldsymbol{\lambda})$. Our results for three canonical compact binaries having three initial eccentricities, $e_t = 0.01, 0.05$ and 0.1 are listed in Table. III. For mildly eccentric binaries, having initial $e_t \sim 0.1$, there are two ways of computing FFs. In the first case, we neglected the existence of the third harmonic which allow us to use Eq. (9) with $\omega = 40\,\pi$Hz while computing n_i. Following Ref. [16], we may include the third harmonic by adding $n/2$ to the right hand side of Eq. (9) and equating it to $40\,\pi$Hz while numerically evaluating n_i. The associated FFs are also given in Table III.

The numbers presented in the Table III, in comparison with the Table. II, clearly indicate that the quasi-circular GW templates, given by Eqs. (19) and (20), are highly efficient in capturing GWs from compact binaries having some residual orbital eccentricity. The higher FFs for massive compact binaries should be due to the fact that they emit stronger GWs and have smaller time window to dephase. Finally, in Fig. 2, we plot $\mathcal{O}(\boldsymbol{\theta})$, the so-called overlap, obtained by maximizing the ambiguity function

TABLE III: The initial-LIGO FFs that uses Eqs. (19) and (20) to model circular GW templates and Eqs. (5) having 2.5PN accurate orbital motion to represent fiducial eccentric GW signals. The symbols m_t and η_t, as expected, denote the total mass and the symmetric mass ratio of the desired template. The initial and final values of ω and n are chosen to have f_{GW} varying between 40 Hz and $(6^{3/2}\,\pi\,Gm/c^3)^{-1}$. For our $m_1 = m_2 = 1.4M_\odot$ binary, the orbital evolution is terminated when the relevant harmonic reaches 1000Hz: the photon shot noise limit. When the initial $e_t = 0.1$, the FFs are computed by including (and neglecting) the third harmonic. We include the effect of the third harmonic by using, for example, $n_i = 78.76$Hz for GWs signals having $m = 11.4$ and $\eta = 0.108$.

$m_1/M_\odot : m_2/M_\odot$		1.4 : 1.4	1.4 : 10.0	10.0 : 10.0
$e_t = 0.01$	FF	0.999	0.999	0.999
	m_t	2.813	11.42	20.16
	η_t	0.248	0.107	0.247
$e_t = 0.05$	FF	0.966	0.993	0.992
	m_t	2.937	11.72	20.40
	η_t	0.233	0.104	0.244
Without the third harmonic				
$e_t = 0.10$	FF	0.894	0.965	0.970
	m_t	3.133	12.71	20.66
	η_t	0.212	0.094	0.244
Including the third harmonic				
$e_t = 0.10$	FF	0.888	0.983	0.984
	m_t	2.833	11.69	20.51
	η_t	0.246	0.102	0.244

over the kinematical variables t_0 and ϕ_0.

To make sure that Eqs. (19) and (20) representing our quasi-circular GW templates, can lead to higher FFs, we performed the following test. It is obvious that dn/dt, given in Eqs. (20), can be written in terms of $\mathcal{M}$ as

$$\frac{dn}{dt} = \frac{96}{5}\left(\frac{G\,\mathcal{M}\,n}{c^3}\right)^{5/3} n^2\,. \tag{21}$$

Therefore, we constructed a set of quasi-circular GW templates that used the same m and η as our PN eccentric GW signal to define $d\phi/dt$, given in Eq. (20). However, we used above equation for dn/dt and treated $\mathcal{M}$ as an independent parameter and computed FFs while maximizing over $\mathcal{M}$ [and this is much simpler procedure than maximizing over m and η]. The resulting FFs turned out to be very close to the entries listed in Table III.

We conclude the section by providing following brief summary of our analysis. When one restricts radiation reaction to the dominant order and wants to model GWs from compact binaries in eccentric orbits, it is appropriate and desirable to employ Ref. [10]. We have demonstrated that certain circular templates, given by Eqs. (19) and (20), representing GWs from compact binaries inspiralling under quadrupolar radiation reaction along 2PN accurate circular orbits, are efficient in capturing our fiducial GW signals from eccentric binaries. The crucial difference between the various circular templates, considered as the cases I, II and III,and the case VI is that the Eqs. (19) and (20), representing the case VI, treat

FIG. 2: The overlap for a binary system with $m_1 = 1.4M_\odot$, $m_2 = 10.0M_\odot$ and initial $e_t = 0.1$ in the m_t - η_t space. It is visually rather difficult to pinpoint a global maximum. However, for a large number of (m_t, η_t) values, the overlap is more than 0.92.

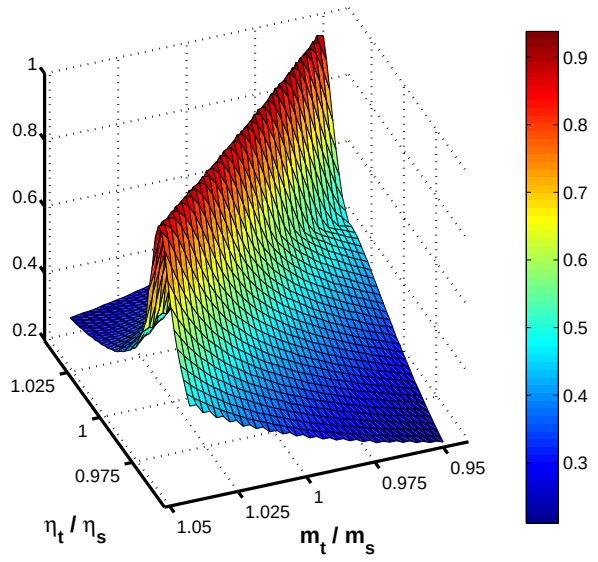

the conservative and reactive orbital phase evolution in a gauge-invariant manner with equal emphasis.

V. CONCLUDING DISCUSSIONS

We explored the drops in the signal-to-noise-ratios, relevant for the initial LIGO, while non-optimally searching for GWs from compact binaries inspiralling under quadrupolar radiation reaction along PN accurate eccentric orbits with various types of circular templates. The fiducial GW signals are somewhat realistically modeled with the help of Ref. [10], that provided $h_{\times,+}|_Q(t)$ from inspiralling eccentric binaries having 2.5PN accurate adiabatic phase evolution. We demonstrated that search templates obtained by perturbing compact binaries in 2PN accurate circular orbits with dominant order reactive dynamics are highly efficient in capturing our GW signals even from very mildly eccentric compact binaries. However, the search templates arising from the adiabatic, complete adiabatic and complete non-adiabatic approximants were found to be rather inefficient in capturing the fiducial GW signals having even tiny residual orbital eccentricities. In our view, the present analysis indicates that it is desirable to treat, in an equal footing, both the conservative and reactive contributions to the orbital phase evolution, while constructing the search templates for GWs from astrophysical compact binaries.

We are aware that the various kinds of PN accurate search templates for the quasi-circular inspiral, available in LAL [8], employ directly or indirectly Eq. (3a) and

different prescriptions for the PN-accurate reactive evolution of $x(t)$. Therefore, it will be rather important to extend our present analysis to investigate if various quasi-circular search templates, employed by the GW data analysts, can capture GW signals from compact binaries inspiralling along eccentric orbits and, say, having 3PN accurate conservative and 2PN accurate reactive dynamics. For such an analysis, the construction of PN accurate GW signals from inspiralling eccentric binaries should be influenced by Refs. [10, 15] and this is currently under active investigation. Further, while providing more accurate prescriptions to compute GW signals from eccentric binaries, it is imperative to include currently neglected contributions due to $\tilde{c}_\alpha$, appearing at 2.5 and 3.5PN orders. We also feel that such post Newtonian accurate versions of the present analysis should be repeated for VIRGO, Advanced LIGO and LISA. It is also desirable to explore the effects of the spins on the present FF computations. This requires construction of GW signals from spinning compact binaries inspiralling along PN accurate eccentric orbits building on a preliminary investigation presented in Ref. [25].

Acknowledgments

We are very grateful to Gerhard Schäfer for detailed discussions and encouragements. We thank anonymous referee and Eric Poisson for their opinions. This work is supported in part by the grants from the DFG (Deutsche Forschungsgemeinschaft) through SFB/TR7 "Gravitationswellenastronomie" and the DLR (Deutsches Zentrum für Luft- und Raumfahrt).

APPENDIX A: 2PN ACCURATE ORBITAL DYNAMICS FOR ECCENTRIC BINARIES

In this appendix, we provide explicit 2PN accurate parametric expressions for $r, \dot{r}, \phi$ and $\dot{\phi}$ in harmonic gauge, required to construct $h_{\times,+}|_Q(t)$ from inspiralling eccentric binaries having 2.5PN accurate orbital motion. These parametric expressions are extracted from Eqs. (23)-(26) in Ref. [15]. The radial motion, parametrically defined by $r(l, n, e_t)$ and $\dot{r}(l, n, e_t)$, reads

$$r = r_{\rm N} + r_{\rm 1PN} + r_{\rm 2PN}\,, \tag{A1a}$$
$$\dot{r} = \dot{r}_{\rm N} + \dot{r}_{\rm 1PN} + \dot{r}_{\rm 2PN}\,, \tag{A1b}$$

where

$$r_{\rm N} = \left(\frac{GM}{n^2}\right)^{1/3}(1 - e_t\cos u)\,, \tag{A2a}$$
$$r_{\rm 1PN} = r_{\rm N}\times\frac{\xi^{2/3}}{6(1-e_t\cos u)}[-18 + 2\eta - (6-7\eta)e_t\cos u]\,, \tag{A2b}$$
$$r_{\rm 2PN} = r_{\rm N}\times\frac{\xi^{4/3}}{72(1-e_t^2)(1-e_t\cos u)}\Big\{-72(4-7\eta) + \left[72 + 30\eta + 8\eta^2 - (72 - 231\eta + 35\eta^2)e_t\cos u\right](1-e_t^2) - 36(5-2\eta)(2+e_t\cos u)\sqrt{1-e_t^2}\Big\}\,, \tag{A2c}$$
$$\dot{r}_{\rm N} = \frac{(GMn)^{1/3}}{(1-e_t\cos u)}e_t\sin u\,, \tag{A2d}$$
$$\dot{r}_{\rm 1PN} = \dot{r}_{\rm N}\times\frac{\xi^{2/3}}{6}(6-7\eta)\,, \tag{A2e}$$
$$\dot{r}_{\rm 2PN} = \dot{r}_{\rm N}\times\frac{\xi^{4/3}}{72(1-e_t\cos u)^3}\Big[-468 - 15\eta + 35\eta^2 + (135\eta - 9\eta^2)e_t^2 + (324 + 342\eta - 96\eta^2)e_t\cos u + (216 - 693\eta + 105\eta^2)(e_t\cos u)^2 - (72 - 231\eta + 35\eta^2)(e_t\cos u)^3 + \frac{36}{\sqrt{1-e_t^2}}(1-e_t\cos u)^2(4-e_t\cos u)(5-2\eta)\Big]\,, \tag{A2f}$$

The angular motion, describable using PN accurate parametric expressions for ϕ and $\dot{\phi}$, is given by

$$\phi(\lambda, l) = \lambda + W(l)\,, \tag{A3a}$$
$$\lambda = (1+k)l\,, \tag{A3b}$$
$$W(l) = W_{\rm N} + W_{\rm 1PN} + W_{\rm 2PN}\,, \tag{A3c}$$
$$\dot{\phi} = \dot{\phi}_{\rm N} + \dot{\phi}_{\rm 1PN} + \dot{\phi}_{\rm 2PN}\,, \tag{A3d}$$

The above mentioned various PN quantities read

$$k = \frac{3\xi^{2/3}}{1-e_t^2} + \frac{\xi^{4/3}}{4(1-e_t^2)^2}\left[78 - 28\eta + (51-26\eta)e_t^2\right]\,, \tag{A4a}$$
$$W_{\rm N} = v - u + e_t \sin u\,, \tag{A4b}$$
$$W_{\rm 1PN} = \frac{3\xi^{2/3}}{1-e_t^2}(v - u + e_t \sin u)\,, \tag{A4c}$$
$$W_{\rm 2PN} = \frac{\xi^{4/3}}{32(1-e_t^2)^2(1-e_t\cos u)^3}\Bigg(8\left[78 - 28\eta + (51-26\eta)e_t^2 - 6(5-2\eta)(1-e_t^2)^{3/2}\right](v-u)(1-e_t\cos u)^3\,, \tag{A4d}$$
$$\dot{\phi}_{\rm N} = \frac{n\sqrt{1-e_t^2}}{(1-e_t\cos u)^2}\,, \tag{A4e}$$
$$\dot{\phi}_{\rm 1PN} = \dot{\phi}_{\rm N} \times \frac{\xi^{2/3}}{(1-e_t^2)(1-e_t\cos u)}\left[3 - (4-\eta)e_t^2 + (1-\eta)e_t\cos u\right]\,, \tag{A4f}$$
$$\begin{aligned}\dot{\phi}_{\rm 2PN} = \dot{\phi}_{\rm N} \times \frac{\xi^{4/3}}{12(1-e_t^2)^2(1-e_t\cos u)^3}\Bigg\{&144 - 48\eta - (162 + 68\eta - 2\eta^2)e_t^2 + (60 + 26\eta - 20\eta^2)e_t^4 + (18\eta + 12\eta^2)e_t^6 \\ &+ \left[-216 + 125\eta + \eta^2 + (102 + 188\eta + 16\eta^2)e_t^2 - (12 + 97\eta - \eta^2)e_t^4\right]e_t\cos u + \left[108 - 97\eta - 5\eta^2\right. \\ &\left.+(66 - 136\eta + 4\eta^2)e_t^2 - (48 - 17\eta + 17\eta^2)e_t^4\right](e_t\cos u)^2 + \left[-36 + 2\eta - 8\eta^2 - (6 - 70\eta - 14\eta^2)e_t^2\right](e_t\cos u)^3 \\ &+ 18(1-e_t\cos u)^2(1 - 2e_t^2 + e_t\cos u)(5-2\eta)\sqrt{1-e_t^2}\Bigg\}\,.\end{aligned} \tag{A4g}$$

In the circular limit, it is not that difficult to conclude that the 2PN accurate expression for $\dot{\phi}$ becomes

$$\dot{\phi} = n\left\{1 + 3\,\xi^{2/3} + \left(\frac{39}{2} - 7\,\eta\right)\xi^{4/3}\right\}. \tag{A5}$$

The above equation, in terms of k, is simply $\dot{\phi} = n\,(1+k)$. Therefore, while using n and in the limit $e_t \to 0$, deviations from the Newtonian accurate orbital motion may be explained in terms of k. However, this explanation is representation dependent as shown below.

Using PN accurate expressions, given in Ref. [14], one can easily represent in the circular limit $\dot{\phi}$ using the conserved orbital energy and it reads

$$\dot{\phi} = \frac{\zeta^{3/2}}{G\,m}\left\{1 + \frac{1}{8}\left[9 + \eta\right]\frac{\zeta}{c^2} + \left[\frac{891}{128} - \frac{201}{64}\,\eta + \frac{11}{128}\,\eta^2\right]\frac{\zeta^2}{c^4}\right\}, \tag{A6}$$

where $\zeta = -2\,E/\eta\,m$ and E being the conserved center-of-mass orbital energy. While employing ζ, it is obvious that deviations from Newtonian accurate phase evolution can not be explained purely in terms of k.

A comparison of Eqs. (A5) and (A6) leads to the following observations. Using the usual definition $\dot{\phi} = \omega = 2\,\pi/T$ and Eq. (A6), one may define a PN accurate period T. However, at PN orders, this is not given by $T_r = 2\,\pi/n$, the radial period of Keplerian type parameterization and the period relevant to construct GW signals from inspiralling eccentric binaries. The above defined T is related to n by $T = \frac{2\,\pi}{n\,(1+k)}$. Further, observe that there are various PN accurate ways of defining ω and they, at a given GW phasing order, lead to various quasi-circular GW templates.

[1] B. Abbott *et al.* [LIGO Scientific Collaboration], [arXiv:gr-qc/07040943].

[2] S. Hild [LIGO Scientific Collaboration], Class. Quant. Grav. **23**, S643 (2006).

[3] F. Acernese *et al.*, Class. Quant. Grav. **23**, S635 (2006).

[4] T. Damour, P. Jaranowski, and G. Schäfer, Phys. Lett. B **513**, 147 (2001); L. Blanchet, G. Faye, B. R. Iyer, and B. Joguet, Phys. Rev. D **65**, 061501(R) (2002); **71**, 129903(E) (2005); L. Blanchet, T. Damour, G. Esposito-Farèse, and B. R. Iyer, Phys. Rev. Lett. **93**, 091101 (2004); K. G. Arun, L. Blanchet, B. R. Iyer, and M. S. S. Qusailah, Class. Quant. Grav. **21**, 3771 (2004); **22**, 3115(E) (2005) and references therein.

[5] P.C. Peters, Phys. Rev.**136**, B1224 (1964).

[6] K. Martel and E. Poisson, Phys. Rev. D **60**, 124008 (1999)

[7] H. K. Chaurasia and M. Bailes, Astrophys. J. **632**, 1054 (2005); K. L. Page *et al.*, Astrophys. J. **637**, L13 (2006); J. Grindlay, S. P. Zwart, and S. McMillan, Nature (London) **2**, 116 (2006).

[8] *Lsc algorithm library (LAL)*, `http://www.lsc-group.phys.uwm.edu/lal`; T. Damour, B. R. Iyer and B. S. Sathyaprakash, Phys. Rev. D **63** (2001) 044023 [Erratum-ibid. D **72** (2005) 029902] [arXiv:gr-qc/0010009].

[9] P. Ajith, B. R. Iyer, C. A. K. Robinson and B. S. Sathyaprakash, Phys. Rev. D **71**, 044029 (2005) [Erratum-ibid. D **72**, 049902 (2005)] [arXiv:gr-qc/0412033].

[10] T. Damour, A. Gopakumar, and B. R. Iyer, Phys. Rev. D **70**, 064028 (2004).

[11] T. Damour and N. Deruelle, Ann. Inst. Henri Poincaré Phys. Théor. **44**, 263 (1986).

[12] T. Damour and G. Schäfer, Nuovo Cimento Soc. Ital. Fis., B **101**, 127 (1988).

[13] G. Schäfer and N. Wex, Phys. Lett. **174 A**, 196, (1993); erratum **177**, 461.

[14] R.-M. Memmesheimer, A. Gopakumar, and G. Schäfer, Phys. Rev. D **70**, 104011 (2004).

[15] C. Königsdörffer and A. Gopakumar, Phys. Rev. D **73**, 124012 (2006).

[16] M. Tessmer and A. Gopakumar, Mon. Not. Roy. Astron. Soc. **374**, 721 (2007) [arXiv:gr-qc/0610139].

[17] P. Colwell, *Solving Kepler's Equation Over Three Centuries*, Willman-Bell, Inc. (1993).

[18] S. Mikkola, *Celestial Mechanics*, **40**, 329 - 334, (1987).

[19] T. A. Apostolatos, Phys. Rev. D **52**, 605 (1995).

[20] B. J. Owen, Phys. Rev. D **53**, 6749 (1996) [arXiv:gr-qc/9511032].

[21] W. H. Press, W. T. Vetterling,S. A. Teukolsky and B. P. Flannery, *Numerical Recipes in C++: the art of scientific computing*, Cambridge University Press, (2002).

[22] T. Damour, B. R. Iyer and B. S. Sathyaprakash, Phys. Rev. D **57**, 885 (1998) [arXiv:gr-qc/9708034].

[23] L. Blanchet, B. R. Iyer, C. M. Will, and A. G. Wiseman, Class. Quant. Grav. **13**, 575 (1996).

[24] L. Blanchet, T. Damour, and B. R. Iyer, Phys. Rev. D **51**, 5360 (1995).

[25] C. Königsdörffer and A. Gopakumar, Phys. Rev. D **71**, 024039 (2005).